Progress In Electromagnetics Research C, Vol. 56, 163–172, 2015

CLEAN Deconvolution Applied to Passive Compressed Beamforming

Thomas Fromenteze*, Ettien Kpre, David Carsenat, and Cyril Decroze

Abstract—In this article, a matching pursuit algorithm is developed to improve the performance of a passive multiplexing technique based on compressed sensing. This deconvolution technique is applied to RADAR imaging in the microwave range, starting from previous studies based on a compact coding device and L^1-norm regularizations. This study demonstrates that in this context, the quality of the reconstructed RADAR images can be improved using an algorithm close to Hogbom's Clean, and based on a dictionary built with Tikhonov pseudo-inversions. The theoretical principle of this new algorithm is developed, followed by a parameters study. Finally, an experimental validation is presented to demonstrate the efficiency of this iterative algorithm.

1. INTRODUCTION

In the current context of development of microwave systems capable of high resolution imaging, the complexity and price of the required active UWB (Ultra WideBand) devices are the main obstacles to the large scale implementation of these technologies. To overcome these limitations, Reference [1] introduces a novel technique able to achieve the multiplexing of waveforms in a passive way. Thus, the active hardware required to achieve imaging can be reduced regardless of the number of antennas. A coding device is used to convolve by pseudo-orthogonal codes and sum the waves received by an antenna array, compressing all the information into a single waveform measured by a unique receiving chain (Fig. 1). In post-processing, all the signals can be reconstructed using pseudo-inversion techniques to finally compute a radar image. In [2, 3], a similar technique is presented based on an aperture made of coupled resonators. In this case, the radiating structure codes spatially the information. However, since both methods can be developed using the same mathematical formulation, the proposed algorithm should be compatible to these works too.

The quality of the RADAR images computed with this method depends on two parameters: the deconvolution technique used for the reconstruction of the waveforms and the correlation between the coding device's channels, which must be as low as possible to prevent inter-signals projection. The aim of this article is to present an iterative approach to improve this reconstruction compared to direct pseudo-inversion techniques. Thus, a matching pursuit algorithm is presented to achieve the reconstruction of these compressed waveforms and to be able to get better RADAR images. The proposed approach is a modified version of Hogbom's Clean algorithm, initially developed for the radio astronomy domain [5, 6] and used for a wide range of application such as the compensation of UWB multipath channels [7] and the angle of arrival detection [8]. In a context of RADAR imaging, this algorithm is usually applied to deconvolve images by the radiation patterns of the device [9]. Here, the algorithm is directly used on the received signals to reduce the complexity and the computation time [10]. Instead of using a dictionary based on match filtered correlations, Tikhonov pseudo-inversions are used to compute a bank of elementary signals composing the received waveforms. In the next section, the signal processing related to this new technique is presented. Then, a parameter study is developed for a numerical simulation of RADAR imaging. Finally, this technique is applied to measured waveforms to confirm its validity.

Received 18 January 2015, Accepted 19 March 2015, Scheduled 24 March 2015
* Corresponding author: Thomas Fromenteze (thomas.fromenteze@unilim.fr).
The authors are with the Xlim Research Institute, University of Limoges, France.

2. THE CLEAN-TIKHONOV ALGORITHM

According to Fig. 1, the expression of the signal measured at the unique output of the coding device is:

$$y(t) = \sum_{n=1}^{N} s(n,t) \otimes h(n,t) + b(\sigma_b, t), \tag{1}$$

where $s(n,t)$ is the signal received by the nth antenna, $h(n,t)$ the channel of the coding device linking this antenna to the common output, and $b(\sigma_b, t)$ the Gaussian additive noise of standard deviation σ_b. The symbol $\otimes$ stands for the convolution operator. This method of measurement is closely related to the principle of compressed sensing: a projection onto a set of orthogonal sub-spaces is achieved by multiplying the data by a sparse matrix, allowing for a compressed sampling of the scene [11].

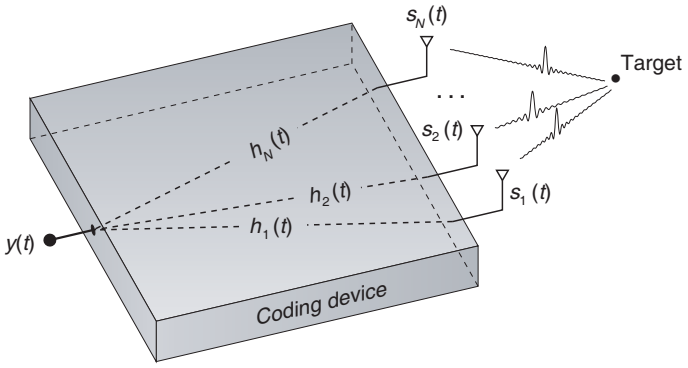

Figure 1. Illustration of a compressive device: the waves received by an antenna array are convolved by channel impulse responses and summed at the common output port.

2.1. Initial Reconstruction: The Tikhonov Regularization

If the channels of the coding device are known and stationary, a deconvolution of the unique measured signal is computed to get an estimation of the waveforms received by the antenna array. Thus, [4] introduces the use of the Tikhonov regularization in this purpose. This L^1-norm regularization is equivalent to a least-square pseudo-inverse with a regularization parameter that prevents the inversion of low values and limits the impact of ill-conditioning. In the frequency domain, the expression of the Tikhonov pseudo-inverse of the matrix $[H(f)]$ is defined by the following equation:

$$[H(f)]^+ = ([H(f)][H(f)]^\dagger + \beta[I])^{-1}[H(f)]^\dagger \tag{2}$$

where β is the regularization parameter, I an identity matrix, and $\dagger$ the transpose-conjugate operator.

Thus, an estimation of the received waveforms $S^+(k,f)$ is computed by multiplying the measured signal in the frequency domain (obtained by a Fourier transform of Eq. (1)) by the Tikhonov pseudo-inverses:

$$S(k,f)^+ = \underbrace{\left(\sum_{n=1}^{N} S(n,f)H(n,f) + B(\sigma_b, f)\right)}_{Y(f)} H^+(k,f). \tag{3}$$

Under the hypothesis of ideally uncorrelated channels and noise-free measurement, the estimation $S(k,f)^+$ would perfectly match the received signals $S(k,f)$. In a realistic situation, the channels of the coding device are bandwidth-limited, so they cannot be perfectly orthogonal and noise can be added to the measurement. Thus, the regularization parameter β is optimized to achieve the best reconstruction [4]. As an illustrative example, Fig. 2 shows the reconstruction of four received RADAR signals compressed into a unique waveform. These signals are obtained by a *Matlab* simulation of a RADAR scene presented in Section 3 and the channels of the coding device developed in [4].

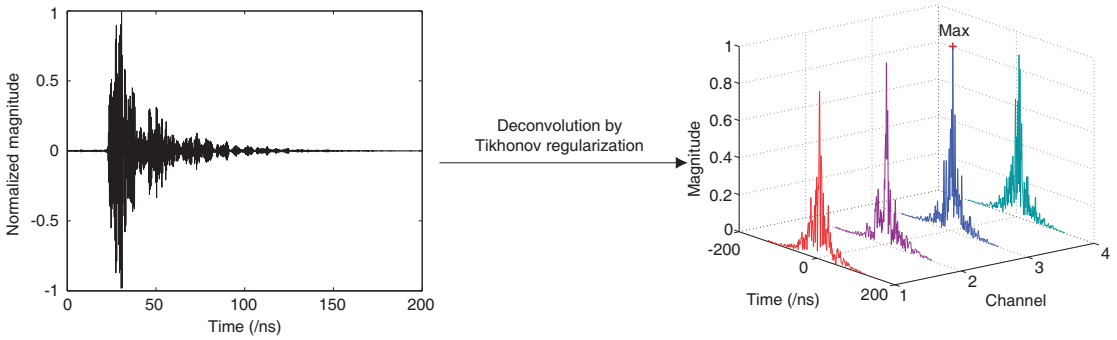

Figure 2. (a) The signal measured at the coding device's output is deconvolved using a Tikhonov regularization to get an estimation of (b) the signals received by the antenna array. The maximum signal is identified for the next step of the algorithm.

The reconstruction of the signal $S(k,f)^+$ received by the kth antenna is obtained by distributing the corresponding pseudo-inverse:

$$S(k,f)^+ = \sum_{n=1}^{N} S(n,f) \underbrace{H(n,f)H^+(k,f)}_{R_{nk}(f)} + B(\sigma_b,f)H^+(k,f), \tag{4}$$

with $R_{nk}(f)$, the correlation between channel n and Tikhonov pseudo-inverse k. These correlations depend on the channels orthogonality and represent the main obstacle in the signals reconstruction. To mitigate the impact of these correlations and reconstruct signals that are closer to the received waveforms, an iterative deconvolution is then performed.

2.2. Iterative Deconvolution Using CLEAN Algorithm

For the next step of the algorithm, a time domain conversion is computed using an inverse Fourier transform:

$$s(k,t)^+ = \sum_{n=1}^{N} s(n,t) \otimes r_{nk}(t) + b(\sigma_b,t) \otimes h^+(k,t) \tag{5}$$

For each iteration, the maximum level of matrix $|[s(t)^+]|$ is identified. It corresponds to the elementary response of a target received by the antenna array, convolved by the compressive device, and finally equalized by the Tikhonov regularization. It leads to k_{Max} the index of the maximum signal and τ_{Max} its corresponding maximum time. Then, the matrix $[s(t)^+]$ is subtracted by the weighted correlation matrix $[r_{n,k_{\text{Max}}}(t)]$ to remove the contribution of this elementary source:

$$[s(t)^+]_{i+1} = [s(t)^+]_i - \alpha \left[r_{n,k_{\text{Max}}}(t-\tau_{\text{Max}})\right] \exp(-j\xi) \tag{6}$$

with:

- $[s(t)^+]_{i+1}$ the matrix $[s(t)^+]$ after $i+1$ iteration.
- α the loop gain, a constant real value set between 0 and 1.
- $\xi = \angle s(k_{\text{Max}}, t-\tau_{\text{Max}})^+|_i$ the phase of the maximum signal, at the maximum time, and at the ith iteration.

At each step, a matrix $[s_{\text{clean}}(t)]$ is incremented by the deconvolved elementary targets' signatures:

$$s_{\text{clean}}\left(k_{\text{Max}}, t-\tau_{\text{Max}}\right)|_{i+1} = s_{\text{clean}}\left(k_{\text{Max}}, t-\tau_{\text{Max}}\right)|_i + \alpha\delta\left(t-\tau_{\text{Max}}\right)\exp(j\xi) \tag{7}$$

The phase ξ of $s(k_{\text{Max}}, t-\tau_{\text{Max}})^+|_i$ is conserved in order to reconstruct complex signals required to achieve the post-processing beamforming and compute microwave radar images. Fig. 3 presents an illustration of the iterative deconvolution.

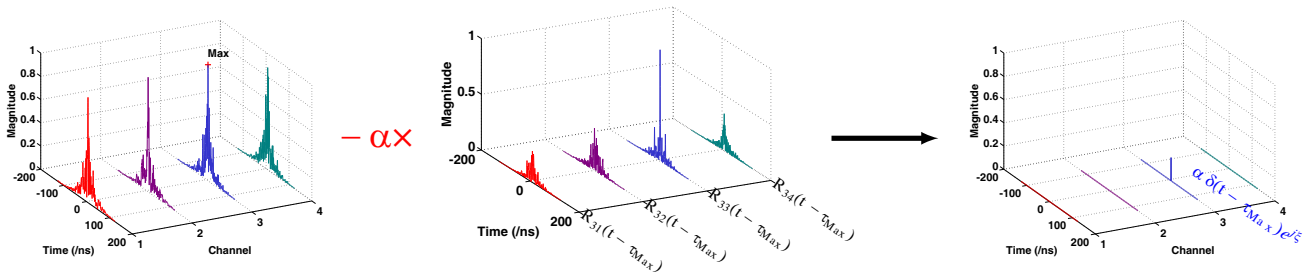

Initial reconstruction

Figure 3. Once the maximum value of the reconstructed signals has been identified, they are subtracted by a set of time-shifted correlations computed with the Tikhonov pseudo-inverses. The aim of this subtraction is to iteratively remove each elementary brick of the signals and to identify them by incrementing new deconvolved signals.

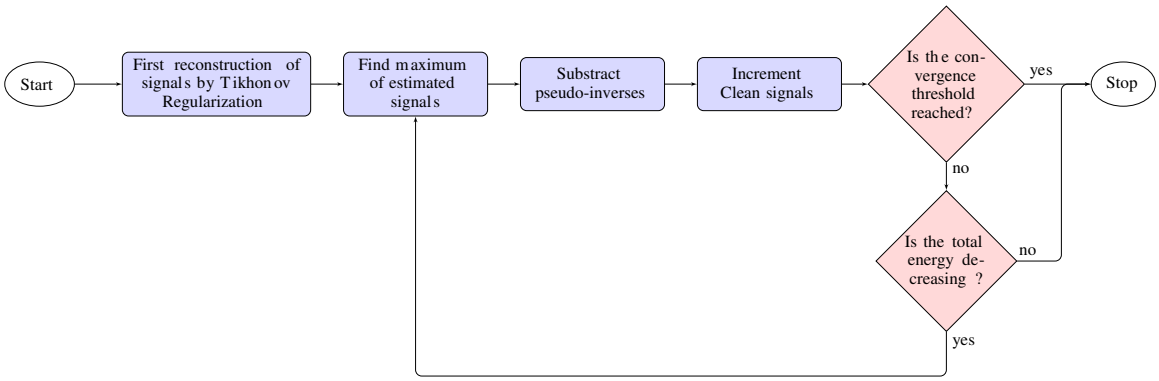

Figure 4. Flow chart of the proposed Clean-Tikhonov algorithm.

A criterion ϵ is defined to stop the loop when the total energy of the signals $[s(t)^+]_{i+1}$ is low enough. Thus, for each iteration the following equation must be satisfied:

$$\sum_{n}^{N} \left| s(n,t)_{i+1}^{+} \right|^2 < \epsilon \tag{8}$$

This parameter has been empirically optimized and is set to $\epsilon = 10^{-3}$ for each application of the algorithm in this paper. A second stopping criterion is defined to prevent the total energy $\sum_n^N |s(n,t)_{i+1}^+|^2$ to increase between two successive iterations. This security is added to prevent the detection of peak values corresponding to noise components. A flow chart is depicted in Fig. 4 to summarize the Clean-Tikhonov algorithm.

In the next section, this deconvolution technique is applied to the 1×4 compressive device introduced in [4]. A simulation is computed with measured channels and confronted to experimental measurements to demonstrate the efficiency of this algorithm.

3. APPLICATION TO A FOUR-CHANNELS COMPACT DEVICE

3.1. Simulation with the Device Measured Channels

The compressing device used for this experience is a photonic crystal made of a periodic pattern engraved on the upper metallic part of a ceramic laminate (Fig. 5). This component is designed to maximize the modal diversity in a compact volume.

In a *Matlab* simulation, an antenna array made of four isotropic elements is connected to the coding component and used in reception. A transmission antenna is set in the middle of the array. The

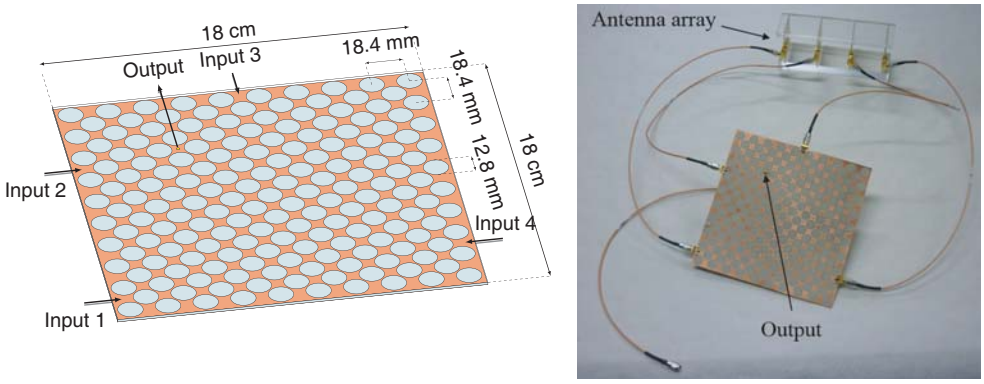

(a) (b)

Figure 5. Coding device issued from [4] used to compress the waves received by an antenna array. The aim of the Clean-Tikhonov algorithm is to perform the reconstruction of the signals received by the array.

Table 1. Data used for the Matlab simulation of a Radar measurement compressed with the coding device.

Number of points	$2^{14} = 16348$
Frequency range	1–4 GHz
Number of R_x antennas	4
Distance between R_x antennas	7 cm
Processor	6×3.50 GHz

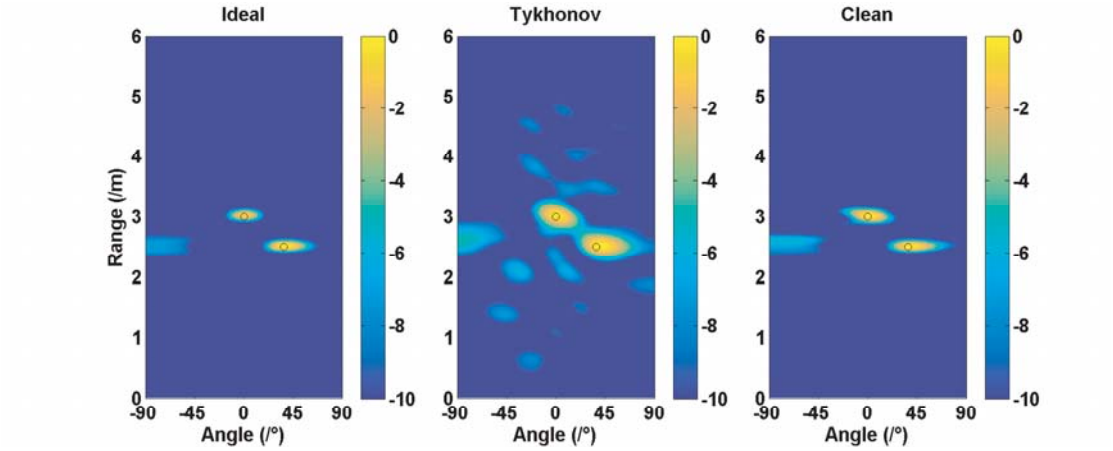

Figure 6. Application of the Clean-Tikhonov algorithm to a simulated scenario: the left picture shows the ideal detection without any compression of signals, the central picture is the result of the first Tikhonov deconvolution and the right picture is the result of the Clean-Tikhonov algorithm.

variables related to the simulation are summarized in Table 1.

Two isotropic targets are set at the coordinates (1.5, 2) and (0, 3). Using free space 2D Green's functions and the Born's first approximation, the signals reflected on the targets are computed at the location of the reception array. Finally, they are coded by the component's channels and summed following Eq. (1). Radar images are computed for three cases (Fig. 6): first, an ideal case without compression is considered. In this case, all the signals received by the antenna array are directly measured, without any compression. Secondly, the radar image obtained using a Tikhonov regularization

is presented. This case corresponds to the initial step of the Clean-Tikhonov algorithm. Finally, the result of the actual algorithm is depicted. The energy threshold is set at $\epsilon = -30\,\mathrm{dB}$ and is reached after 200 iterations in 5.3 s with $\alpha = 10^{-2}$ and $\beta = 0.55$. Conventional delay-and-sum beamforming algorithm was used for each radar image computation. The result of the Clean-Tikhonov algorithm is almost identical to the ideal case.

The peak signal-to-noise ratio between the ideal and the Clean-Tikhonov cases is computed to get a quantitative value of likelihood:

$$\mathrm{PSNR} = 20\log_{10}\left(\frac{Max}{\sqrt{\mathrm{MSE}}}\right), \tag{9}$$

with Max the maximum value of the radar images, and MSE the mean square error defined by the following equation:

$$\mathrm{MSE} = \frac{1}{\theta r}\sum_{m_\theta=1}^{\theta}\sum_{m_r=1}^{r}\left[M_{\mathrm{ideal}}(m_\theta, m_r) - M_{CT}(m_\theta, m_r)\right]^2, \tag{10}$$

with:

- $M_{\mathrm{ideal}}(m_\theta, m_r)$ and $M_{CT}(m_\theta, m_r)$ the radar images computed respectively for the ideal and the Clean-Tikhonov cases.
- θ the discretized angle vector of index m_θ.
- r the discretized range vector of index m_r.

Since both images have been normalized, the maximum value of the images is Max = 1 for each case. Thus, the computed PSNR for this first simulated case is $-47.7\,\mathrm{dB}$.

The efficiency of the deconvolution is presented depending on the regularization parameter β and of the loop gain α. An optimized value of β is a way to improve the initial reconstruction. If $\beta \to +\infty$, the Tikhonov regularization tends matched filtering, corresponding to a conventional Clean algorithm. The results of this study are depicted in Fig. 7.

For this simulation, the optimal deconvolution is computed in 7.05 s (297 iterations) for $\alpha = 7\cdot10^{-3}$, $\beta = 0.55$, leading to a PSNR $= -48.4\,\mathrm{dB}$. Depending on the deconvolution step, the number of iterations required to reach the convergence can be high, involving a long computation time. However, this study shows that using an optimized regularization, the deconvolution step can be chosen high while maintaining good performances. Thus, a PSNR of $-48.15\,\mathrm{dB}$ is obtained for $\alpha = 0.1$, $\beta = 0.55$, in 0.1 s (21 iterations). All these results obviously depend of the complexity of the scene to image but in

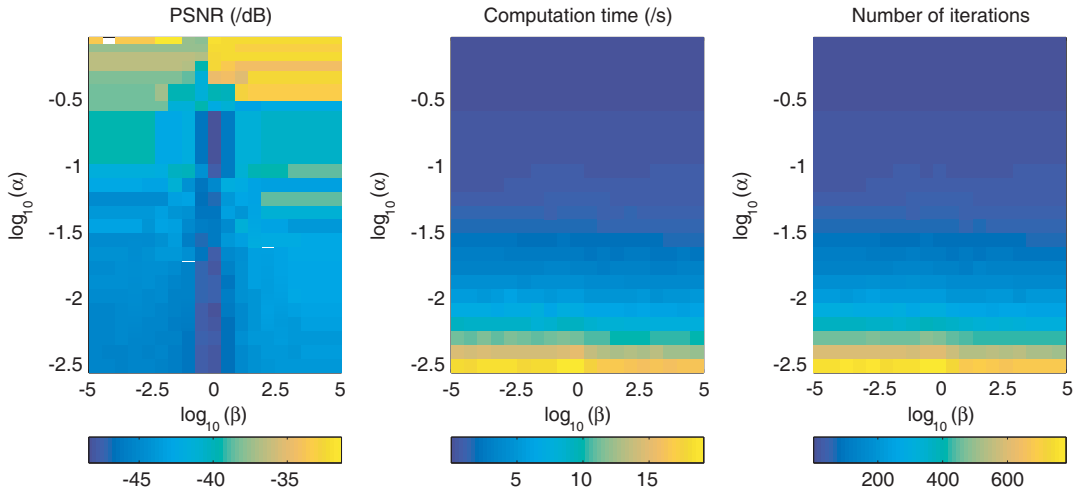

Figure 7. Efficiency of the Clean-Tikhonov algorithm depending on the regularization parameter β and of loop gain α.

every case, the Tikhonov regularization can ensure a faster deconvolution than using the conventional matched filtered correlations since the initial reconstruction and the elementary signals of the matching pursuit are improved.

The next part of this study concerns the impact of the noise on the convergence of the algorithm. Thus, a Gaussian additive noise of standard deviation σ_b is added to the received signal. Since the algorithm is based on the detection of the maximum level of the signals reconstructed, the value detected after several subtractions could belong to a noise component leading to an inefficient deconvolution step. Thus, it could cause the total energy ϵ to increase and to stop the algorithm. To illustrate this phenomenon, an example is computed using the previous scenario and adding a Gaussian additive noise $B(\sigma_b, f)$ to the measured signal in order to modify the SNR. Thus, the standard deviation σ_b is deduced:

$$\sigma_b = \frac{\sigma_{\text{signal}}}{\sqrt{\text{SNR}}} \tag{11}$$

For the same scenario, the algorithm is applied with different levels of SNR. The number of iterations computed for each level is depicted in Fig. 8.

This figure shows that for a constant loop gain α, the amount of iterations is higher for a high SNR, leading to a better radar image. Indeed, when a maximum value corresponding to a noise peak is detected, the subtraction is more likely to increase the total energy implying a stop of the algorithm. To show the inefficiency of the algorithm when a peak component is detected, Fig. 9 presents the evolution of the PSNR when a certain amount of iterations with increasing energy are allowed.

Regardless of the SNR, the PSNR is never improved when components of noise are detected, even if the total energy is decreasing. For the next section of this article, an experimental validation is presented to confirm the validity of the proposed Clean-Tikhonov algorithm.

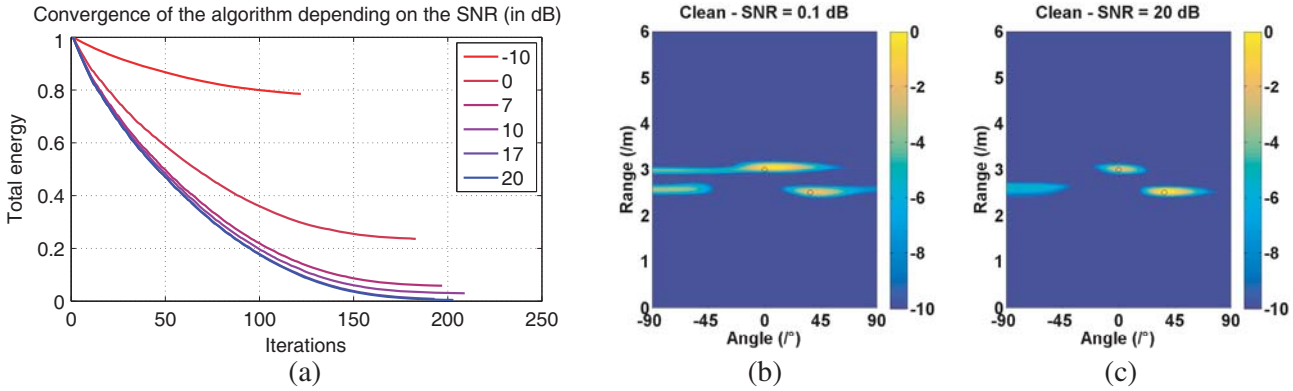

Figure 8. (a) Convergence of the algorithm depending on the SNR. (b) Radar image for SNR = 0.1 dB (PSNR = −36.9 dB). (c) Radar image for a SNR = 20 dB (PSNR = −47.4 dB).

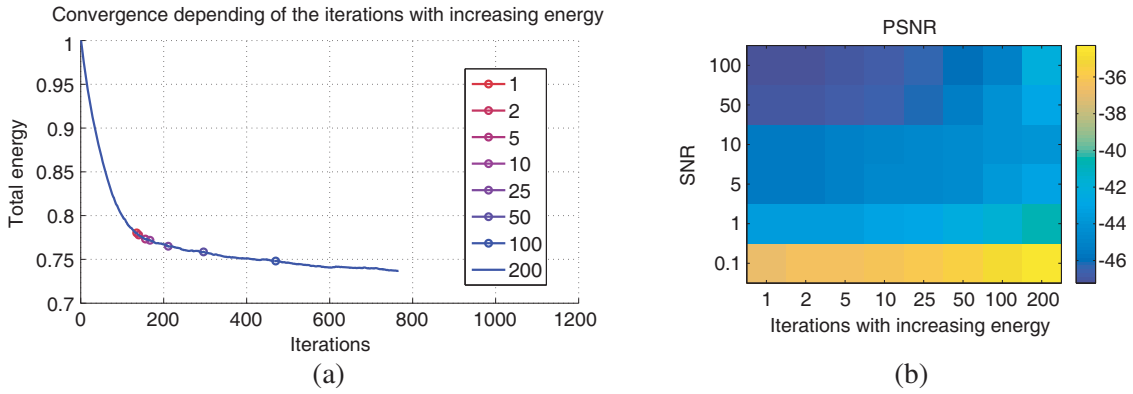

Figure 9. (a) Convergence depending on the amount of allowed iterations with increasing energy for SNR = 0.1 dB. (b) PSNR depending on the amount of iterations with increasing energy.

3.2. Experimental Validation

An experimental bench is installed to match the previous simulations and validate the Clean-Tikhonov algorithm applied to passive imaging. Thus, the data presented in Table 1 are used again, maintaining the same inter-element spacing. Four Vivaldi antennas are connected to the coding device and used in reception while a UWB horn is set in transmission on the right side of the array, at a distance of 50 cm from its center (the path difference is compensated by the delay-and-sum algorithm). The references of the active devices used for the generation and the reception of waves are gathered in Table 2 and the experimental setup is described in Fig. 10.

Table 2. Information related to the experimental setup.

Arbitrary waveform generator	Agilent M8190A 12 GSa/s
Oscilloscope	Agilent DSA90404A 20 GSa/s
Amplifiers	Mini circuits ZVE 8G

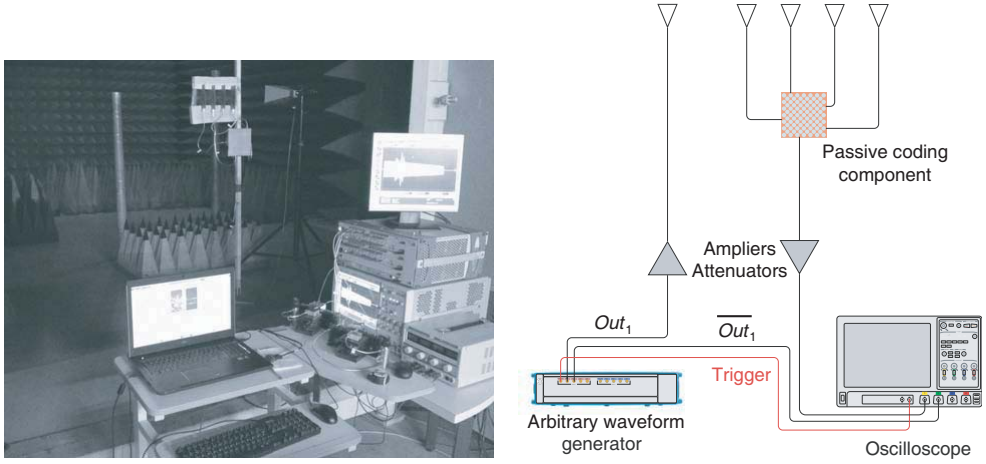

(a) (b)

Figure 10. First step of the proposed algorithm: (a) the signal measured at the coding device's output is deconvoluted using a Tikhonov regularization to get an estimation of (b) the signals received by the antenna array. The maximum signal is identified for the next step of the algorithm.

Two metallic cylinders with isotropic radar cross sections are set in an anechoid chamber and the efficiency of the proposed algorithm is compared to the results obtained using the unique Tikhonov regularization. Since the waveforms to capture are not known, it is not possible to directly compute the SNR of each measurement. For each scenario, two measures are done to compute the standard deviation of the noise. Since the useful signal is common between the two measures, the following equation holds:

$$\sigma^2_{\text{measure}_1-\text{measure}_2} = 2\sigma_b^2 \tag{12}$$

Then, it is possible to compute the SNR of a measurement without knowing the exact useful signal's waveform:

$$\text{SNR} = \frac{\sigma^2_{\text{signal}}}{\sigma_b^2} = \frac{\sigma^2_{\text{total}} - \sigma_b^2}{\sigma_b^2} \tag{13}$$

with:

- σ_{signal}: the standard deviation of the useful signal.
- σ_b: the standard deviation of the noise.
- σ_{total}: the standard deviation of the measured signal.

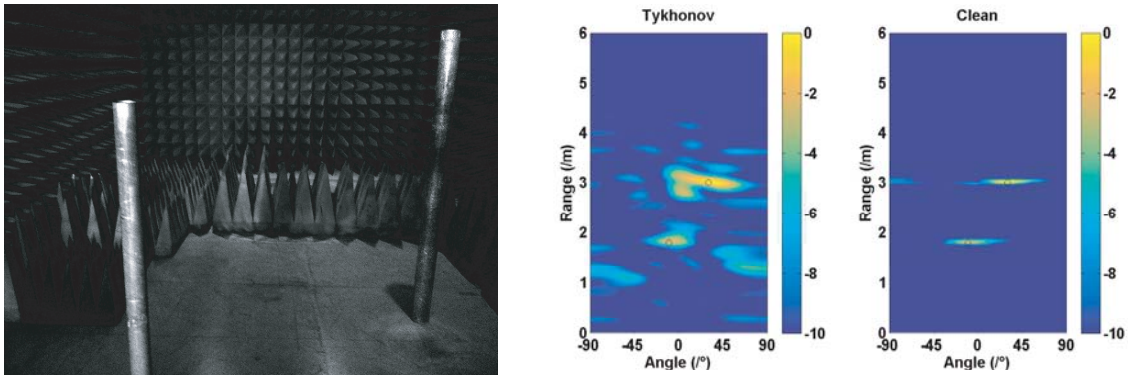

Figure 11. Scenario 1: comparison between a Tikhonov based image and the proposed algorithm.

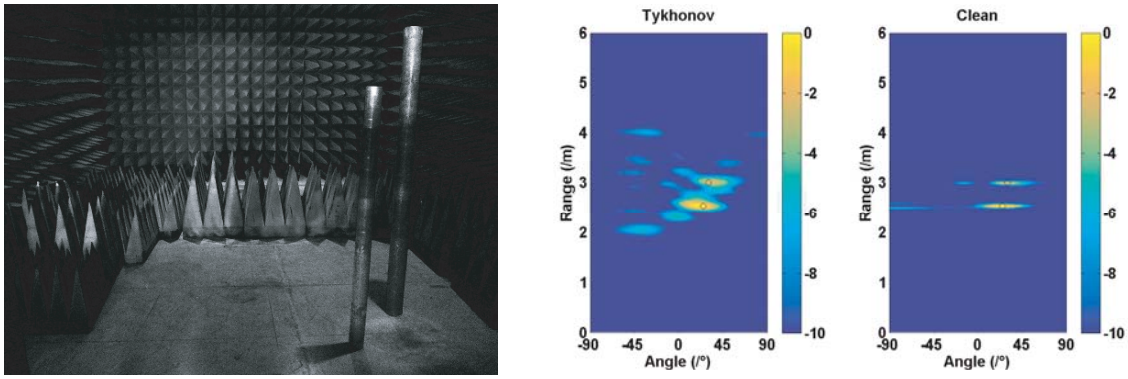

Figure 12. Scenario 2: comparison between a Tikhonov based image and the proposed algorithm.

Figure 11 depicts the first scenario of radar measurement. Black circles are drawn over the computed images to represent the targets' measured positions. For this first case, the Clean-Tikhonov algorithm is computed in 0.79 s (25 iterations), with $\alpha = 0.1$ and $\beta = 0.55$. The SNR of the measured signal is 18.9. Compared to the measured positions, the reconstruction performed with the Tikhonov deconvolution allows for a correct localization of the targets but the side lobes in the time and angular domains prevents from an accurate measurement of their positions. The image obtained with the proposed algorithm is more precise and closer to the ideal case presented in the previous theoretical study. Grating lobes can be observed on the side of the farthest target as in simulation, mostly due to the inter-element spacing. Thus, even if the antenna's' angular-time domain radiation pattern and mutual coupling are not taken into account in the deconvolution, the experimental measurements seems to validate the efficiency of the proposed algorithm. A second scenario is measured by modifying the position of the closest cylinder and putting it next to the second one. The aim of this measurement is to study the convergence of the algorithm when the targets are hard to discriminate using the only Tikhonov regularization. In this case, the SNR of the measured signal is 20.8. The algorithm is computed in 0.7 s (25 iterations), using $\alpha = 0.1$ and $\beta = 0.55$. Once again, the proposed algorithm allows for a better reconstruction of the cylinders' locations.

4. CONCLUSION

An iterative deconvolution algorithm based on the matching pursuit and a dictionary computed Tikhonov pseudo-inverses has been presented. A parameter study is presented to show the efficiency of this algorithm compared to the direct Tikhonov pseudo-inversion introduced in [4] and to matched filtering. It has been shown that quick convergences of the algorithm can be obtained, resulting in RADAR images with reduced time and angular domain side lobes compared to the Tikhonov

regularization. Finally, the proposed algorithm has been experimentally validated with two different scenarii.

Future efforts will be focused on two aspects: First, the potential improvement brought by time domain filters will be studied. Thus, noise components could be eliminated ensuring useful information to be measured, even when the total energy is increasing. Secondly, this algorithm will be confronted to 2D arrays and high-resolution imaging with larger coding devices.

REFERENCES

1. Carsenat, D. and C. Decroze, "UWB antennas beamforming using passive time-reversal device," *IEEE Antenn. Wireless Propag. Lett.*, Vol. 11, 779–782, 2012.
2. Hunt, J., T. Driscoll, A. Mrozack, G. Lipworth, M. Reynolds, D. Brady, and D. R. Smith, "Metamaterial apertures for computational imaging," *Science*, Vol. 339, 310–313, 2013.
3. Lipworth, G., A. Mrozack, J. Hunt, D. L. Marks, T. Driscoll, D. Brady, and D. R. Smith, "Metamaterial apertures for coherent computational imaging on the physical layer," *JOSA A*, Vol. 30, No. 8, 1603–1612, 2013.
4. Fromenteze, T., C. Decroze, and D. Carsenat, "Waveform coding for passive multiplexing: Application to microwave imaging," *IEEE Trans. Antennas Propag.*, Vol. 63, No. 2, 2014.
5. Hogbom, J. A., "Aperture synthesis with a non-regular distribution of interferometer baselines," *Astronomy and Astrophysics Supplement Series*, Vol. 15, 417, 1974.
6. Cornwell, T. J., "Hogbom's CLEAN algorithm. Impact on astronomy and beyond," *Astronomy and Astrophysics*, Vol. 500, 65–66, 2009.
7. Cramer, R. J.-M., R. A. Scholtz, and M. Z. Win, "Evaluation of an ultrawide-band propagation channel," *IEEE Trans. Antennas Propag.*, Vol. 50, No. 5, 561–570, 2002.
8. Akhdar, O., M. Mouhamadou, D. Carsenat, C. Decroze, and T. Monediere, "A new CLEAN algorithm for angle of arrival denoising," *IEEE Antenn. Wireless Propag. Lett.*, Vol. 8, 478–481, 2009.
9. Tsao, J. and R. D. Steinberg, "Reduction of sidelobe and speckle artifacts in microwave imaging: The CLEAN technique," *IEEE Trans. Antennas Propag.*, Vol. 36, 543–556, 1988.
10. Fry, R. D. and D. A. Gray, "CLEAN deconvolution for sidelobe suppression in random noise radar," *IEEE International Conference on Radar*, 209–212, 2008.
11. Candes, E. J. and T. Tao, "Near-optimal signal recovery from random projections: Universal encoding strategies," *IEEE Transactions on Information Theory*, Vol. 52, No. 12, 5406–5425, 2006.